

Shear Reinforcement Spacing in Wide Members

by Adam S. Lubell, Evan C. Bentz, and Michael P. Collins

Large, wide beams and thick slabs are frequently used as transfer elements where the total structural depth must be kept to a minimum. While these members provide large cross-sectional areas of concrete to resist shear demands, shear reinforcement may still be required. For these wide members, design codes do not provide guidance on appropriate limits for spacing of the shear reinforcement legs across the member width. This paper presents the results of 13 new experiments designed to investigate the influence of this spacing on the one-way shear capacity of wide reinforced concrete members. The capacity of members with well-distributed shear reinforcement could be safely predicted by the ACI 318 shear model, but stirrup efficiency decreased significantly as the stirrup leg spacing across the width increased. Limits are proposed on the spacing of stirrup legs across the member width to ensure that the shear reinforcement is effective.

Keywords: beams; reinforced concrete; safety; shear; slabs; stirrups.

INTRODUCTION

Many structural framing schemes include the use of wide members to carry direct forces, or to serve as primary transfer elements. For example, in modern high-rise construction, a system of wide beams may provide a simple and economical system to transfer column loads from the tower portion over required column free spaces in the podium or parking areas below. Thick one-way transfer slabs can serve similar roles when the column layout to be transferred is irregular in the plan.

In many of these design situations, the width and height of the concrete cross section will be sufficiently large such that the one-way shear demand can be satisfied by the concrete alone. This configuration would avoid the construction time and expense associated with introducing shear reinforcement in these large members. Recent research,¹⁻⁴ however, has highlighted the difficulty of accurately assessing the shear capacity for large, lightly reinforced wide members without web reinforcement using ACI 318-08,⁵ due to size effects in shear. Size effect refers to the decrease in shear stress at failure observed as member depth increases, for members without web reinforcement.^{4,6} Thus, it has been recommended that stirrups be included in all large members to mitigate size effect in shear and to enhance the member ductility.¹ In other design situations, architectural limitations may require shallower structural depths, thus requiring web reinforcement to cope with the shear demands on the reduced cross section. While shear reinforcement spacing limits measured along the member length are provided in design codes such as ACI 318, few guidelines exist for appropriate limits on the spacing of stirrup legs across the width of the cross section.

Leonhardt and Walther⁷ suggested that the transverse spacing of stirrup legs should be minimized to adequately anchor and suspend the diagonal compression struts associated with the truss model used for shear reinforcement design. The diagonal compression force must flow toward the stirrup legs,⁷ as shown in Fig. 1(a). Anderson and Ramirez⁸ likened

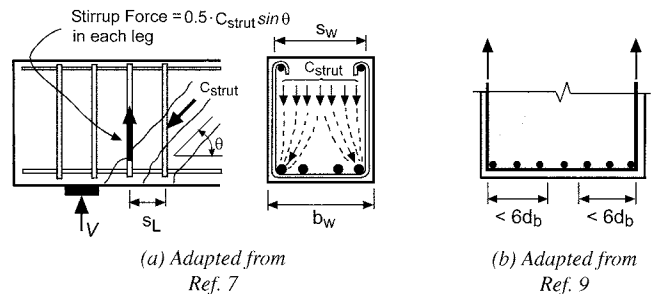


Fig. 1—Force flow analogy in diagonal strut toward shear reinforcement legs: (a) spreading model; and (b) effective strut anchorage width for truss modeling.

this to considering a series of effective truss planes oriented in the longitudinal direction and centered on each line of stirrup legs. An effective width of this plane was not defined,⁸ but detailing rules for strut-and-tie models in the AASHTO LRFD code,⁹ shown in Fig. 1(b), can serve as a guide. These rules suggest that it may no longer be appropriate to consider the web reinforcement as uniformly smeared over the cross section, for members where the legs of the stirrups are spaced further apart than 12 times the bar diameter of the longitudinal reinforcement.

Without specific experimental validation presented, Leonhardt and Walther⁷ suggested a shear reinforcement spacing limit in the width direction of d for low shear stresses, but noted the spacing limit should decrease as a function of the shear stress. For members with high shear stresses, a transverse spacing of 200 mm (7.9 in.) was proposed. In comparison, Leonhardt and Walther⁷ recommended stirrup spacing limits of $0.6d$ or 300 mm (11.8 in.) in the longitudinal direction, with the limits decreased by 50% for shear stresses exceeding approximately $0.135f'_c$. Eurocode 2¹⁰ suggests spacing limits of $0.75d$ or 600 mm (24 in.) in both the width and longitudinal directions. ACI 318-08,⁵ CSA A23.3-04,¹¹ and AASHTO LRFD⁹ limit the spacing in the longitudinal direction to $0.5d$, $0.63d$, and $0.72d$, respectively, but none of these codes provide stirrup leg spacing limits across the width of sections.

Only a small number of studies have directly examined the influence of stirrup spacing across the width on the one-way shear capacity of large members. Hsiung and Frantz¹² performed tests on members up to 457 mm (18 in.) in width using different stirrup configurations and having shear reinforcement ratios approximately 60% higher than the ACI 318-08 minimum limit ($A_v f_y / b_w s_L \sim 0.62 \text{ MPa}$ [90 psi]).

ACI Structural Journal, V. 106, No. 2, March-April 2009.

MS No. S-2007-289 received August 7, 2007, and reviewed under Institute publication policies. Copyright © 2009, American Concrete Institute. All rights reserved, including the making of copies unless permission is obtained from the copyright proprietors. Pertinent discussion including author's closure, if any, will be published in the January-February 2010 ACI Structural Journal if the discussion is received by September 1, 2009.

ACI member **Adam S. Lubell** is an Assistant Professor of Civil Engineering at the University of Alberta, Edmonton, AB, Canada. He received his PhD from the University of Toronto, Toronto, ON, Canada. He is a member of ACI Committees 440, Fiber Reinforced Polymer Reinforcing; 544, Fiber Reinforced Concrete; E803, Faculty Network Coordinating Committee; Joint ACI-ASCE Committee 445, Shear and Torsion; and Task Group ITG-6, High-Strength Steel Reinforcement. His research interests include the design and rehabilitation of reinforced and prestressed concrete structures, and the development of structural detailing guidelines to allow for the use of high-performance materials.

ACI member **Evan C. Bentz** is an Associate Professor of Civil Engineering at the University of Toronto. He is a member of ACI Committee 365, Service Life Prediction, and Joint ACI-ASCE Committee 445, Shear and Torsion. His research interests include the mechanics of reinforced concrete, service life modeling, and the creation of practical tools that transfer reinforced concrete research into the engineering community.

Michael P. Collins, FACI, is University Professor and Bahen-Tanenbaum Professor of Civil Engineering at the University of Toronto. He is a member of Joint ACI-ASCE Committee 445, Shear and Torsion. His research interests include the development of rational and consistent shear design specifications for structural concrete applications.

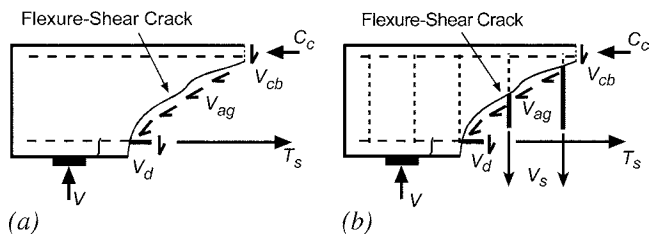


Fig. 2—Sectional model for force transfer at flexure-shear cracks: (a) members without stirrups; and (b) members with stirrups.

Specimens had width-to-height aspect ratios (b_w/h) from 0.33 to 1.0. Higher web reinforcement strains in interior stirrup legs were reported, but the stirrup leg spacing across the width, ranging from $d/4$ to d , did not result in discernible changes in ultimate shear capacity or differences in crack widths measured across the specimen width. Anderson and Ramirez⁸ tested members 406 mm (16 in.) deep, with $b_w/h = 1.0$ and sectional shear stresses of approximately 60% of ACI 318-08 maximum limits ($A_v f_y / b_w s_L \sim 2.14$ MPa [310 psi]). They concluded that the stirrup spacing limits proposed in Reference 7 were appropriate for members subject to high shear stresses. Serna-Ros et al.¹³ tested beams 750 mm (29.5 in.) wide and 250 mm (9.8 in.) high, with different web reinforcement configurations ($A_v f_y / b_w s_L \sim 0.76$ MPa [110 psi]). They concluded that capacity predictions using the ACI 318 model could be improved by adjusting the web reinforcement fraction V_s of the total one-way shear capacity V_n by the ratios $\sqrt{(d/s_L)}$ and $\sqrt{(d/s_w)}$, where s_L and s_w represent the spacing of the web reinforcement legs in the longitudinal and width directions, respectively. Earlier tests on reinforced concrete shells at the University of Toronto with rectilinear patterns of shear reinforcement showed that the shear capacity decreased as the spacing across the width increased for constant shear reinforcement ratios.¹⁴ A staggered pattern of web reinforcement of shear studs was found to improve the performance of cyclically loaded shells with superimposed in-plane tension and compression by preventing excessive transverse splitting along the longitudinal reinforcement and by improving the confinement of the concrete core.¹⁵

The present study was designed to examine the relationship between one-way shear capacity and shear reinforcement spacing across the width for members with large b_w/h aspect ratios. These can be considered as wide beams, or as design strips taken from one-way slabs or large shell structures. A primary objective was to establish appropriate spacing limits

for which the existing ACI 318 modified truss model for sectional one-way shear would produce safe predictions of member capacity. The research focused on members with shear reinforcement ratios close to the ACI 318 minimum requirements, consistent with the relatively low levels of shear stress that would typically be encountered in wide members within building-type structures.

RESEARCH SIGNIFICANCE

Shear reinforcement legs for one-way shear must be appropriately spaced along the member length and across the member width. While spacing limits are provided in design codes for the longitudinal direction, little guidance is available for spacing across the width. Laboratory test results for members up to 1170 mm (46.1 in.) wide are presented, where the web reinforcement pattern within the cross section was a primary test parameter. This study proposes new guidelines for the maximum transverse spacing of shear reinforcement to ensure adequate safety of wide members designed using the ACI 318-08 truss model for one-way shear.

ROLE OF WEB REINFORCEMENT

Shear failures in slender flexural members are associated with the formation of inclined cracks.¹⁶ After the diagonal cracks form, the structure relies on the transfer of forces across this division to maintain equilibrium. Thus, it is important to understand the force transfer mechanisms so that adequate levels of safety are achieved.

In a slender diagonally cracked member without web reinforcement (Fig. 2(a)), resistance to shear is provided by the uncracked compression block, V_{cb} ; aggregate interlock along the crack surface, V_{ag} ; and dowel action from the longitudinal reinforcement, V_d .¹⁶ Most design code models for shear^{5,9-11} do not attempt to isolate each mechanism, but instead provide a strength term to estimate the equivalent combined action of all three modes. Indeed, ACI 318-08⁵ design provisions use an empirical estimate of the force to cause significant diagonal cracking as a proxy to the mechanisms described previously.¹⁷ The commonly used ACI 318-08 expression for one-way shear capacity of a member without web reinforcement, which is subject to flexure and shear, is (ACI 318-08, Eq. (11-3))

$$V_c = 0.166 \sqrt{f'_c} b_w d \quad (\text{MPa, mm units}) \quad (1a)$$

$$V_c = 2 \sqrt{f'_c} b_w d \quad (\text{psi, in. units}) \quad (1b)$$

where f'_c is the compressive strength of concrete cylinders, b_w is the web width, and d is the effective depth of the longitudinal tensile reinforcement measured from the compression face.

When web reinforcement is introduced, the behavior after the formation of a principal diagonal crack is considerably more ductile. Based on truss models originally developed by Ritter¹⁸ and Mörsch,¹⁹ the ACI 318 model⁵ estimates the direct contribution to shear capacity from the web reinforcement, V_s , using a 45-degree truss analogy (ACI 318-08, Eq. (11-15))

$$V_s = \frac{A_v f_y t d}{s_L} \quad (2)$$

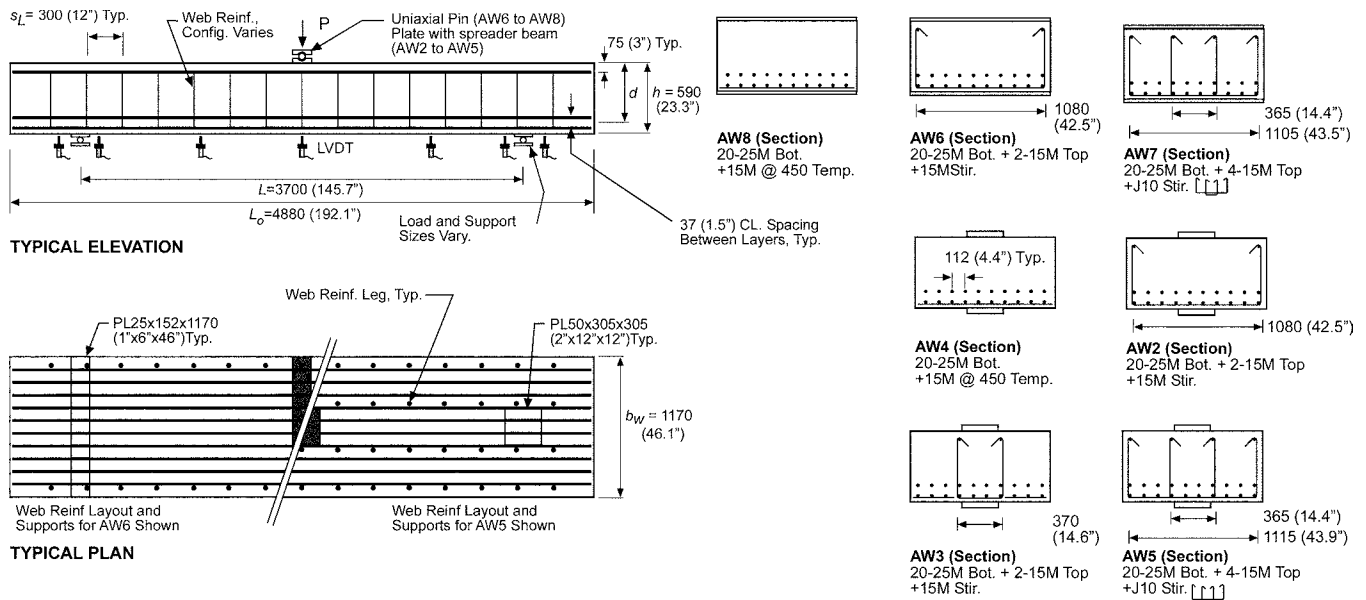


Fig. 3—AW Series specimen configuration.

where A_v is the area of web reinforcement within a cross section taken perpendicular to the member longitudinal axis, and f_{yv} is the yield strength of the web reinforcement. Equation (2) assumes that all shear reinforcement within an averaged distance of $\pm 0.5d$ of the critical section for shear will have reached the yield strength at the time of shear failure.

Joint ACI-ASCE Committee 326¹⁷ recognized that members with web reinforcement tested in the laboratory were consistently stronger than the predictions developed from Eq. (2) alone. Furthermore, at loads after cracking but prior to failure, stirrup strains were lower than would be predicted from the truss model alone. Thus, the ACI 318-08 modified truss model for shear relies on the observation that test results of narrow members containing well-distributed web reinforcement can be safely predicted by the summation of a mechanics-based truss component V_s , with the empirically derived diagonal cracking load, V_c

$$V_n = V_c + V_s \quad (3)$$

While Eq. (3) is convenient for design, the actual force transfer mechanisms can be more readily represented by Fig. 2(b).¹⁶ In addition to forces carried directly through the web reinforcement (V_s in Fig. 2(b)), the force transfer mechanisms corresponding to the compression block, V_{cb} ; aggregate interlock, V_{ag} ; and dowel action, V_d , are enhanced from the corresponding values in a geometrically identical member without web reinforcement.¹⁶ Well-detailed web reinforcement will provide confinement to the compression block, control crack widths (and thereby enhance aggregate interlock on the crack surfaces), and control splitting action along the longitudinal bars from dowel action. Thus, it is reasonable to assume that the magnitude of V_c in Eq. (3) would be sensitive to the web reinforcement arrangement if taken by the customary interpretation as concrete contribution rather than the originally defined diagonal cracking load. Both the AASHTO LRFD⁹ and CSA¹¹ codes assume that the introduction of minimum web reinforcement mitigates the size effect in shear for the V_c component. For this assumption to be accurate, the web reinforcement must be sufficiently

well distributed over the member cross section to control crack widths.

EXPERIMENTAL INVESTIGATION

Experiments were conducted on reinforced concrete wide beams and slab strips as part of a larger study on shear in wide reinforced concrete members.³ This paper reports the results of 13 specimens in two different series, where each series was established by nominal specimen dimensions. The specimens were intended to be full-scale models of typical wide beams and slab strips and contained web reinforcement ratios consistent with the relatively low levels of shear stress that would be encountered in wide beams and slabs within building structures. Shear reinforcement spacing was a primary test variable.

It is important to note that in the verification of Eq. (3), ACI Committee 326¹⁷ examined the results of 166 experiments and found an average ratio of V_{test}/V_n of 1.44 with a coefficient of variation of 23.7%. With the analytical model having this degree of conservatism and scatter, it is difficult to determine if the spacing of the web reinforcement is excessive by just comparing the observed failure shear to the ACI 318 predicted failure shear. This study uses companion specimens that did not contain web reinforcement as an additional basis of comparison. If adding widely spaced shear reinforcement has little effect on the shear strength of a member compared to the companion, then presumably the spacing of the web reinforcement is excessive.

Specimen configuration

The seven specimens in the AW series, which are described in Fig. 3 and Table 1, were constructed to nominal dimensions of 1170 mm (46.1 in.) width, 590 mm (23.2 in.) total height, and 4880 mm (192.1 in.) total length. The specimens were tested under three-point bending with a central span of 3700 mm (145.7 in.), giving a shear span-depth ratio (a/d) of approximately 3.65. Four of these specimens, AW2, AW3, AW4, and AW5, were loaded and supported via 305 x 305 mm (12 x 12 in.) steel plates to simulate column loads and column supports. The other three specimens, AW6,

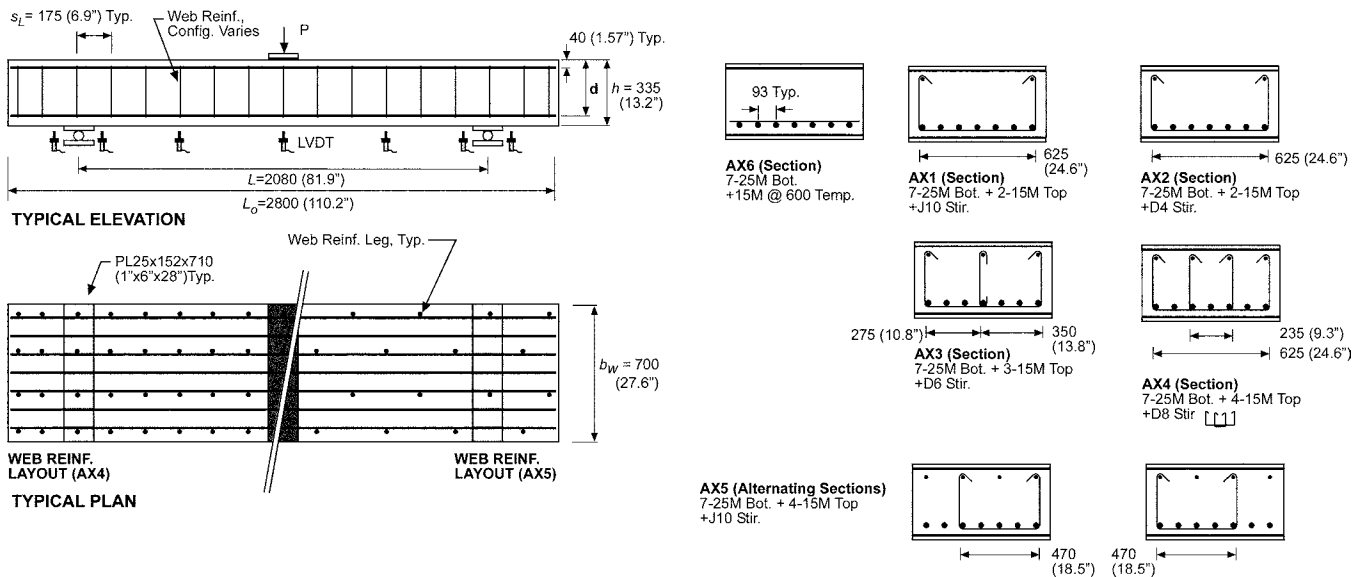


Fig. 4—AX Series specimen configuration.

Table 1—AW specimen properties and test results

Specimen	b_w , mm	h , mm	d , mm	a/d	f'_c , MPa	ρ	$A_v f_{yt} / b_w s_L$, MPa	s_w , mm	s_w/d	V_{test} , kN	ϵ_{long} at V_{test} , $\mu\epsilon$	Δ_{max} at V_{test} , mm	$V_s^*_{exp} / V_{s,ACI}$	$V_{test} / V_{n,ACI}$	
Narrow load and support conditions															
AW2		1172	591	507	3.65	39.3	1.68	0.514	1080	2.13	818	1858	10.31	0.305	0.88
AW3		1165	593	509	3.63	37.2	1.69	0.517	800	1.57	837	1902	9.01	0.365	0.92
AW4		1168	590	506	3.66	39.9	1.69	—	—	—	725	1561	6.39	—	1.17
AW5		1170	590	511	3.62	34.8	1.67	0.355	375	0.73	963	2268	13.23	1.122	1.20
Full-width load and support conditions															
AW6		1169	593	509	3.63	43.7	1.68	0.515	1080	2.12	841	1876	9.29	0.134	0.87
AW7		1170	591	512	3.61	35.8	1.67	0.355	370	0.73	1074	2366	14.69	1.288	1.33
AW8		1169	591	507	3.65	39.4	1.69	—	—	—	800	1710	7.75	—	1.29

Note: V_{test} represents applied shear force (including specimen self-weight and apparatus weight) at ACI 318 critical section for beam shear d for edge of support plate; s_w represents maximum spacing between adjacent stirrup legs in same cross section; 1 mm = 0.0394 in.; 1 MPa = 145.04 psi; and 1 kN = 0.2248 kips.

AW7, and AW8, were loaded and supported by full-width plates to simulate wall loads and wall supports. The five AW specimens with web reinforcement had stirrups spaced at 300 mm (11.8 in.) along the length of the member. That is, s_L was approximately $0.59d$. This spacing was chosen because it seemed likely that members where the longitudinal spacing of the stirrups was close to the maximum permitted by various codes would be more sensitive to any detrimental effects of wide spacing across the width of the member. Web reinforcement patterns included four legs across the width, two legs near the specimen edges, and two legs concentrated within a central column-strip. It is important to note that the arrangement with four stirrup legs across the width resulted in a stirrup clamping stress parameter, $(A_v f_{yt}) / (b_w s_L)$, only 69% as great as that produced by the two-stirrup-leg arrangements (refer to Table 1). All seven of the AW specimens had the same longitudinal reinforcement, resulting in a ρ_w ratio of 1.68%. This relatively high percentage was chosen so that the calculated flexural failure load exceeded the nominal ACI 318 shear failure load by

approximately 40%, thus making flexural failure unlikely. Top longitudinal bars used to anchor the stirrups varied, but would have minimal influence on overall member response.

The six AX series specimens, which were all loaded and supported with full width plates, are described in Fig. 4 and Table 2. Nominal dimensions for the specimens were 700 mm (27.6 in.) width, 335 mm (13.2 in.) total height, and 2800 mm (110.2 in.) total length. The central span was 2080 mm (81.9 in.), giving $a/d = 3.65$. The smaller dimensions for the AX specimens were chosen so that a wider variety of web reinforcement configurations could be investigated within the scope of the project. The five AX specimens with web reinforcement had stirrups spaced at 175 mm (6.9 in.) along the member length ($s_L = 0.61d$) and contained either two, three, or four web reinforcement legs across the width. Corresponding differences in the leg diameter or yield strength of the web reinforcement gave similar values for the stirrup clamping stress parameter in all specimens (refer to Table 2). Specimen AX5 used stirrups with two legs across

Table 2—AX specimen properties and test results

Specimen	b_w , mm	h , mm	d , mm	a/d	f'_c , MPa	ρ_s , %	$A_v f_{yt} / b_w s_L$, MPa	s_w , mm	s_w/d	V_{test} , kN	ϵ_{long} at V_{test} , $\mu\epsilon$	Δ_{max} at V_{test} , mm	$V_{s,exp}^* / V_{s,ACI}$	V_{test} / V_n	
AX1		703	339	289	3.60	42.0	1.72	0.506	625	2.16	460*	5623	12.25	1.718	1.43
AX2		703	336	286	3.64	42.0	1.74	0.502	625	2.19	340	2090	5.56	0.564	1.07
AX3		707	335	285	3.65	42.0	1.74	0.574	350	1.23	452*	3466	11.10	1.457	1.35
AX4		698	335	285	3.65	42.0	1.76	0.527	235	0.82	417	2625	9.59	1.276	1.30
AX5		697	333	283	3.67	41.0	1.77	0.511	470	1.66	361	2385	7.85	0.772	1.16
AX6		703	338	288	3.61	41.0	1.73	—	—	—	283	1673	4.24	—	1.31

*Strain gauge results indicate some yielding of some longitudinal reinforcement.

Notes: V_{test} represents applied shear force (including specimen self-weight and apparatus weight) at ACI 318 critical section for beam shear d for edge of support plate; s_w represents maximum spacing between adjacent stirrup legs in same cross section; 1 mm = 0.0394 in.; 1 MPa = 145.04 psi; and 1 kN = 0.2248 kips.

Table 3—Reinforcement characteristics

Bar no.	A_{bar} , mm ² (in. ²)	f_y , MPa (ksi)	f_u , MPa (ksi)
25M	500 (0.775)	467 (67.7)	637 (92.4)
15M	200 (0.310)	452 (65.6)	618 (89.6)
J10	68.0 (0.105)	458 (66.4)	642 (93.1)
D4	51.6 (0.080)	600 (87.0)	668 (96.9)
D6	38.7 (0.060)	613 (88.9)	660 (95.7)
D8	25.8 (0.040)	625 (90.6)	649 (94.1)

the width, but these stirrups were installed in an alternating pattern (refer to Fig. 4).

Instrumentation for each specimen was designed to capture the load-deformation response, strain in the reinforcing bars, and crack development. Vertical displacement measurements across the width of the members were recorded from linear variable displacement transformers (LVDTs). Deflection values have been corrected for measured settlements occurring at the supports. A system of LVDT-based bulging gauges, which measured the increase in member thickness caused by diagonal cracking, was also installed in the AX specimens (refer to Fig. 5). The holes through the concrete for the bulging gauge were formed with 6 mm (1/4 in.) diameter flexible plastic tubing that was removed prior to the tests. The free movement of the LVDT piston prevented the gauge from acting as a force-resisting element. Applied load, including the weight of the apparatus, was recorded from the machine head. Electrical strain gauges were placed on some longitudinal reinforcement bars in each specimen. Locations were selected to investigate variations in bar forces across the specimen width and along the length. Additional instrumentation details are provided in Reference 3.

Materials

Reinforcement used in the AW series consisted of deformed bars for the longitudinal and web reinforcement. AX specimens used deformed longitudinal bars and deformed bars or deformed wire for the web reinforcement. The properties of the reinforcement are provided in Table 3. Reinforcement bar areas reported are nominal values. Tension coupon tests were used to determine the yield strength from randomly selected samples of each bar stock. The 25M and 15M reinforcing bars exhibited well-defined yield points. The yield point for the J10 reinforcement and the deformed wire were found using the 0.2% offset method.

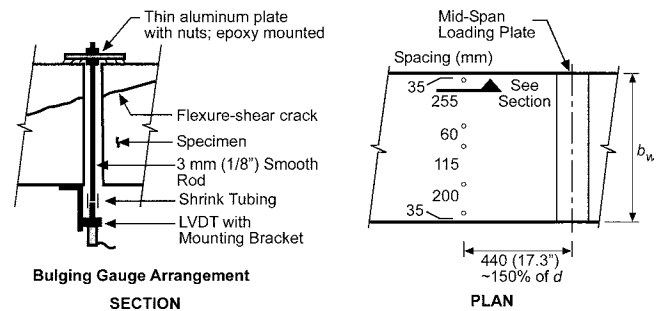


Fig. 5—AX Series bulging gauge configuration.

All AW specimens were cast sequentially in the same plywood formwork over a 10-month period. AX specimens were cast in two sets, approximately 4 weeks apart. Concrete was supplied from a local ready mixed concrete company, contained 9 mm (3/8 in.) coarse aggregate, and had a nominal specified strength of 25 MPa (3.6 ksi). The aggregate was crushed limestone or river gravel for the AW and AX series, respectively. Specimens were cured under moist burlap and plastic for approximately 7 days and then stored in the ambient laboratory conditions prior to testing. Standard 152 x 305 mm (6 x 12 in.) cylinders were cast with the specimens. The average specimen age at testing was approximately 66 days for AW specimens with narrow supports (AW2 to AW5), 217 days for AW specimens with wide supports (AW6 to AW8), and 335 days for the specimens in the AX series. The f'_c values in Tables 1 and 2 represent the average strength of cylinders tested on the same day as the specimen after having been cured under similar laboratory conditions.

Testing procedures

All tests were conducted using a 5400 kN (1200 kip) capacity universal testing machine, where the applied force was controlled through manual operation of the hydraulic valves for the loading piston. Each specimen was loaded in 6 to 11 load increments to failure. At each load stage, the load was decreased by approximately 10% for safety while the cracks were marked, measured with comparator gauges, and photographed. Continuous recording of the load, displacements, and reinforcement strains were provided throughout each test.

Experimental results: AW series

Load-deflection response—Figure 6(a) provides a comparison of the load-deflection relationships for the three

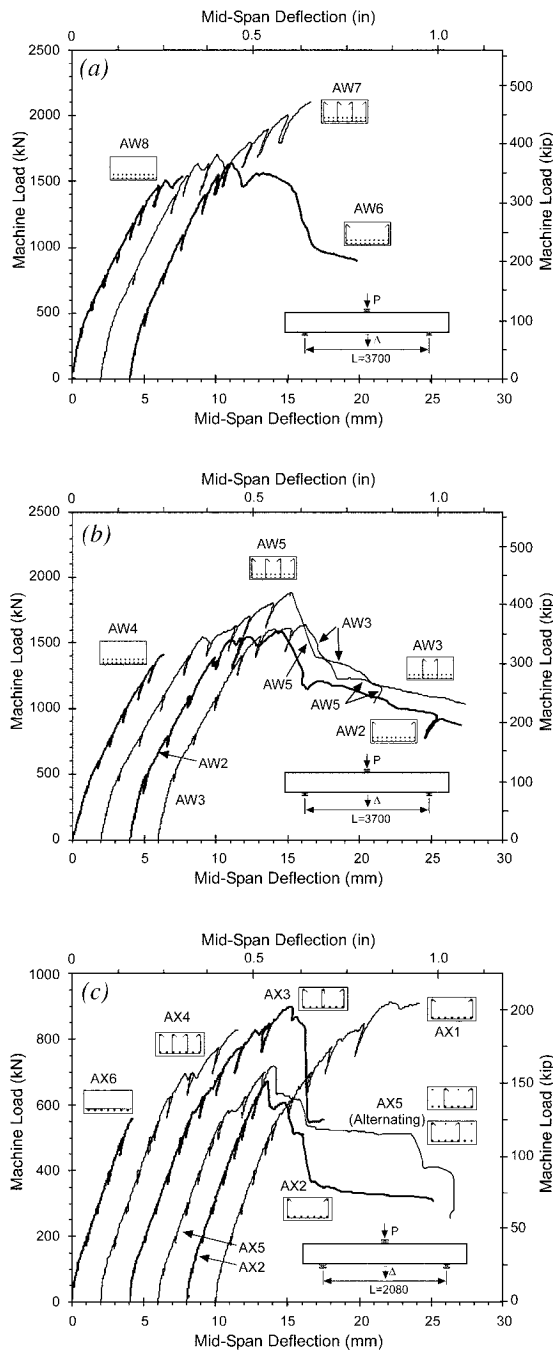


Fig. 6—Load-midspan deflection relationships: (a) AW series with full-width loads and supports; (b) AW series with narrow loads and supports; and (c) AX series with full-width loads and supports.

specimens of the AW series that had full-width loads and supports. A horizontal offset (2 mm [0.08 in.]) of the curves has been used to facilitate comparisons because the three specimens exhibited almost the same load-deflection behavior up to the flexure-shear cracking load, which was very similar for the three specimens. Specimen AW8, without web reinforcement, failed in shear at the formation of the first major diagonal crack. Specimen AW7, with four stirrup legs across the member width ($s_w/d = 0.72$), was able to carry a load 34% higher than AW8, which is close to the increase in shear capacity predicted by ACI 318 for the addition of this quantity of shear reinforcement. The failure of AW7 at the peak load was characterized as brittle, where buckling

of the top reinforcement between the stirrup legs and blowout of the concrete was observed on the top of the east span near the loading point. The corresponding applied load decreased suddenly by 22% from the peak. Specimen AW6 contained 45% more shear reinforcement than AW7 and hence was predicted by ACI 318 to have a shear failure load 55% greater than the specimen with no stirrups (AW8). Because of the wide spacing of the stirrup legs ($s_w/d = 2.12$) in AW6, however, the actual increase in failure load was only approximately 5% compared with AW8 (with no stirrups). While these widely spaced stirrup legs did little to increase the shear failure load, they did make the failure considerably more ductile. The maximum displacement of AW6, shown in Fig. 6(a), was limited by the test setup.

Figure 6(b) provides a comparison of the load-deflection relationships for the four specimens of the AW series that had loads and supports that occupied only 26% of the width of the specimens. It can be seen that for these specimens, the reduction in support and load width has caused the failure loads to be reduced by approximately 10% from the corresponding specimens in Fig. 6(a). This detrimental effect, which is neglected in most codes^{5,9,10,11} is discussed in more detail in Reference 3. Once again, the specimen with the closely spaced stirrup legs, AW5, where $s_w/d = 0.73$, failed at a load approximately 33% higher than the companion specimen with no stirrups (AW4). The specimen with the widely spaced stirrup legs, AW2 ($s_w/d = 2.13$), failed at a shear not much higher than AW4 (with no stirrups). Specimen AW3, which had stirrups arranged within a narrow column strip (refer to Fig. 3), displayed a similar load-deformation response to AW2. Specimens AW2 and AW3 were assigned similar s_w parameters because the maximum transverse spacing in AW3 was assumed from one leg to the location where the next leg would occur in a series of parallel, joined, AW3 strips. For AW2 and AW3, the ACI expressions predict that these two specimens should be 49% and 46% stronger, respectively, than the companion specimen without stirrups, AW4. Because of the wide spacing of the stirrup legs, however, they were only 13% and 15% stronger, respectively, than AW4. Once again, while the widely spaced stirrup legs of AW2 and AW3 were relatively ineffective at enhancing the shear strength, an increase in failure ductility was observed. Specimen AW5 exhibited some post-peak energy absorption, whereas AW4 without stirrups was characterized by a brittle failure. Maximum displacements achieved for AW2, AW3, and AW5 were limited by the test setup.

Crack development—Figure 7 shows the crack patterns after failure for the seven AW specimens. At comparable load levels, the crack patterns and crack widths among the specimens with web reinforcement were qualitatively similar. Furthermore, the crack development was similar on both side faces of the members. Measured widths of cracks prior to failure for the two specimens without web reinforcement (AW4 and AW8) were very small, 0.05 mm (0.002 in.), with brittle failure occurring at or soon after the formation of the principal diagonal crack. On the other hand, Specimen AW7 had measured diagonal crack widths of approximately 4.0 mm (0.157 in.) just prior to the peak load. The corresponding specimen with narrow supports, AW5, exhibited diagonal crack widths of approximately 2.0 mm (0.08 in.). From the specimens with wide U-stirrup configurations, AW6 on full-width supports had crack widths in the region of the failure crack of approximately 0.1 mm (0.004 in.). The peak load was reached soon after the formation of the principal

diagonal crack. In comparison, AW2 on narrow supports had a diagonal crack width of approximately 1.2 mm (0.047 in.) on one shear span just before the peak, but the peak load was reached when a diagonal crack formed in the other shear span. Specimen AW3, which had the same stirrup area as AW2 but with the stirrup legs further from the specimen side faces, had diagonal crack widths of 3.0 mm (0.12 in.) prior to the peak load. It is also noted from Fig. 7 that in the case of narrow loads (AW2 to AW5), the final failure crack extended past the centerline of the specimen, whereas it stopped at the loading plate edge for specimens with full-width loads (AW6 to AW8).

Reinforcement strains—Up to five longitudinal reinforcement bars across the width were instrumented for each AW specimen, and the maximum measured strain value corresponding to the peak machine load is provided in Table 1. For all AW specimens, all longitudinal strain gauges showed a linear response with increasing load, indicating that yielding of the longitudinal reinforcement did not occur.

The results showed that the longitudinal reinforcement will not be evenly strained across the width of a wide member, with different sections showing higher, lower, or similar strains in the outer bars compared with the middle bars. It is noted, however, that local reinforcing bar strain magnitudes are sensitive to the proximity of the nearest crack, which can vary across the width. Strain readings in this study were inconclusive for establishing a strain distribution pattern in relation to location in the span, to the stirrup leg arrangement, or to load and support conditions.

Experimental results: AX series

Load-deflection response—Figure 6(c) provides a comparison of the load-deflection relationships for each of the web reinforcement patterns studied in the AX series, along with the companion specimen that did not contain web reinforcement (AX6). Once again, a horizontal offset of the curves is provided to avoid overlapping the curves. All six specimens exhibited virtually identical load-deflection behavior up to the flexure-shear cracking load, which was similar for all specimens. Specimen AX6, without web reinforcement, suffered an abrupt shear failure at the formation of the first significant diagonal crack. Specimens AX1, AX3, AX4, and AX5 all showed significant increases in peak force capacity beyond the shear cracking load. AX5 had a lower post-cracking stiffness compared with AX1 through AX4, which was attributed to influences on crack development due to the use of a staggered shear reinforcement pattern as compared with a rectilinear grid. The shear cracking load of AX2 was not well defined by the test data, but little additional capacity over the shear cracking load of AX6 was obtained. Nevertheless, a large midspan displacement was achieved with reducing capacity, indicating that the web reinforcement provided additional energy absorbance capacity to the failure mechanism. Indeed, locations of steps in the postpeak response of AX2, AX3, and AX5 in Fig. 6(c) corresponded to audible stirrup rupture, further highlighting the potential ductility improvement of members with web reinforcement in the post-peak range. Rupture and associated necking of stirrups was observed with AX4, where a brittle failure occurred and a sudden 73% decrease in the load from the peak was measured. A nearly total loss of capacity occurred for AX6 (without stirrups) at the brittle failure condition.

Crack development—Figure 8 shows the final crack patterns for the AX series specimens. At comparable load

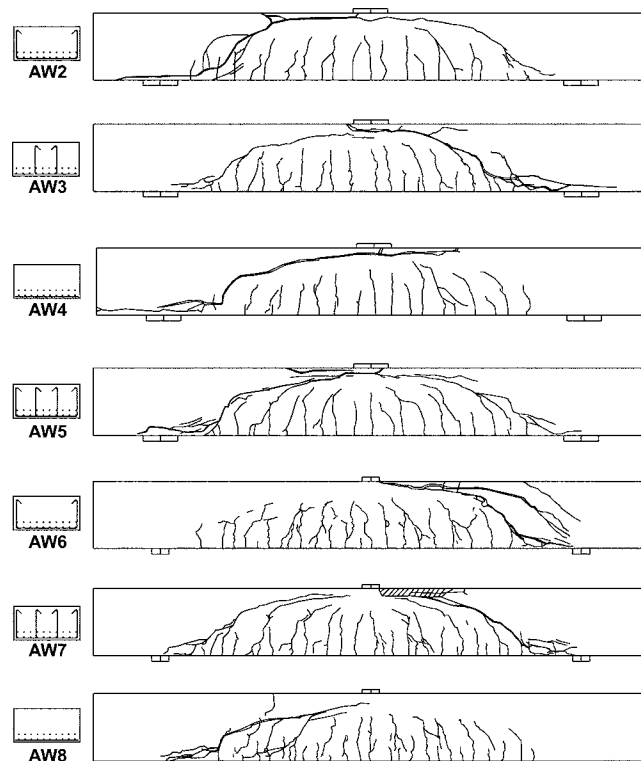


Fig. 7—Crack patterns after failure for AW series specimens.

levels, the crack patterns and crack widths among the AX specimens with symmetrical web reinforcement patterns (AX1, AX2, AX3, and AX4) were qualitatively similar. Crack development was also qualitatively similar for both side faces of the same member. Widths of principal diagonal cracks near the peak load condition for these specimens were typically 0.6 to 1.2 mm (0.024 to 0.047 in.). Specimen AX2 showed crack widths of 0.1 mm (0.004 in.) as compared with AX1 with 0.6 mm (0.024 in.) crack widths, which had a similar web reinforcement pattern. For comparison, the crack widths for AX6 without web reinforcement were approximately 0.05 mm (0.002 in.) at approximately 90% of the failure load.

In the case of AX5, with a staggered pattern of web reinforcement legs, larger cracks were present at load levels near failure, and a difference in crack development was observed in relation to the proximity of the nearest web reinforcement leg to the side face. Diagonal crack widths of 2.5 mm (0.098 in.) were measured on the failure crack on the east side of the specimen at 98% of the failure load. On the west side of AX5, where the stirrup leg at the corresponding cross section was toward the middle of the specimen, maximum diagonal crack widths were approximately 3.0 mm (0.118 in.). In the postpeak region, the cracks on the east face increased slightly, but the cracks on the west side increased to approximately 19 mm (0.75 in.), even while the specimen was maintaining a force capacity of approximately 98% of the peak load. Even for such large crack widths, the postpeak response exhibited reasonable levels of deformation capacity, unlike the brittle failure of AX6 without web reinforcement. Cracks on the specimen soffits were generally perpendicular to the span for most AX specimens. For Specimen AX5, however, the soffit cracks were heavily influenced by the locations where the bottom portions of the U-stirrup were not continuous across the full specimen width (Fig. 9).

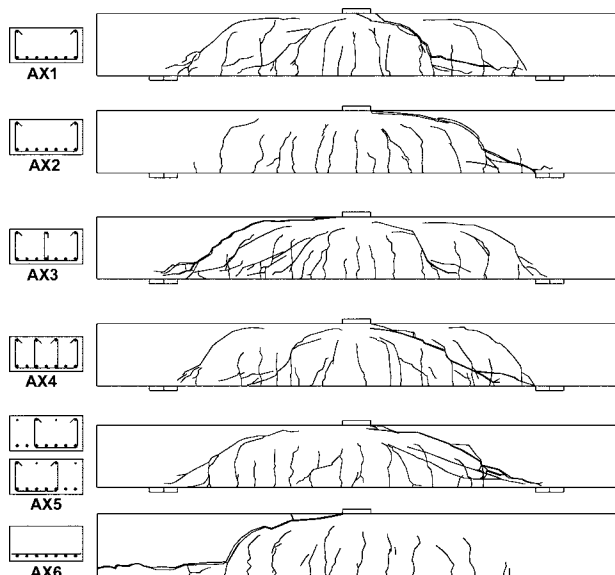


Fig. 8—Crack patterns after failure for AX series specimens.

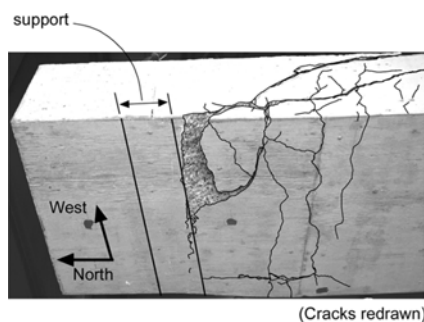


Fig. 9—Soffit cracks for AX5 after failure.

Each of the AX specimens was instrumented with bulging gauges to allow for an estimation of differences in crack widths across the cross section in relation to the stirrup leg configuration (refer to Fig. 5). Of the members with web reinforcement, the flexure-shear crack corresponding to the failure crack intersected the plane of the bulging gauges for AX1 and AX3. Average gauge measurements of approximately 4.0 and 3.3 mm (0.16 and 0.13 in.), respectively, were recorded at the peak machine load, corresponding to approximately 1.3% of d . The gauge measurements were larger than the width of the face cracks because the gauge measurements may reflect the cumulative width of several cracks (refer to Fig. 8). Nevertheless, the readings suggest that the principal diagonal cracks were sufficiently large that the aggregate interlock capacity on the crack face near the failure load would be significantly smaller than that available just after flexure-shear cracking. Near the flexure-shear cracking load, face cracks were small and a large proportion of the total shear could be carried by interlock at this stage. The interlock will decrease, however, as the cracks open at higher load. For the other AX specimens, where the failure crack occurred on the opposite shear span, the bulging gauge measurements were from 0.2 to 1.2 mm (0.008 to 0.047 in.). In all cases, measurements across the specimen width did not differ by more than approximately 10%. This variation appeared consistent with random variations in cracking, and no discernible pattern of crack width across the specimen width or in relation to the web reinforcement patterns was observed.

In AX1, the final failure crack was along a steep flexure-shear crack much closer to the loading plate compared with the other AX specimens. The very high longitudinal strains in AX1, discussed in the following, suggest that the failure mechanism of AX1 cannot be readily modeled using a sectional shear approach. In this regard, it would appear that AX1 is an outlier result, and AX2 would be more typical of the failure condition for the web reinforcement configuration with widely spaced legs. Note that AX1 and AX2 were cast simultaneously. It was also observed that the shape of the AX4 failure crack appeared more linear than the rounded shapes of the other specimens in the AX and AW series, which may account for a capacity slightly lower than what the trends discussed in the following suggest. Overall, the AX series test results suggested a trend of decreasing shear capacity as the web reinforcement spacing s_w increased.

Reinforcement strains—Like the AW specimens, strain gauges affixed to several longitudinal reinforcement bars across the width of each specimen also indicated some variation in strain distribution between the bars along the length. For most AX specimens, middle bars had higher strains compared with outer bars near the support locations, and slightly higher outer bar strains compared with middle bars at midspan, with the variation typically increasing in the postpeak regime. These could not be correlated against discernible patterns in the AW specimens, however, where some specimens had narrow loads and supports. For AX5, the outer bars on the west side showed significantly higher strains near the face of the support, but much lower strains at the quarter-span point. This variation was attributed to the influence of the stirrup pattern on the flexural cracking pattern, as shown in Fig. 9.

Maximum strain values at midspan for the peak applied load are provided in Table 2. It is noted that the maximum strain recorded in AX1 ($5623 \mu\epsilon$) greatly exceeded the maximum yield strain of the longitudinal reinforcement. Thus, AX1 is considered an outlier result for the evaluation of sectional shear capacity. Specimen AX3 had a peak strain in the middle bar at midspan of $3466 \mu\epsilon$, which exceeds the yield strain of the longitudinal reinforcement. The outer bars at midspan, however, had linear strain responses up to strain magnitudes of approximately $2500 \mu\epsilon$ at failure, indicating that only some of the bars had yielded. While the final failure was observed to be by shear, including audible stirrup rupture, the partial yielding of the longitudinal reinforcement suggests that the failure may have been influenced by combined flexure and shear action. The peak machine load for AX3 was approximately 13% above the flexural capacity predicted by ACI 318-08.

INFLUENCE OF STIRRUP LEG SPACING ON SHEAR CAPACITY

As discussed previously, the ACI 318-08 shear model assumes a constant contribution to shear capacity from the concrete (V_c) if web reinforcement is introduced in a member. Thus, according to this model, the influence of the stirrup leg spacing on shear capacity can be determined by comparing the shear strength of a member with web reinforcement against a comparable specimen where the web reinforcement is omitted. A new parameter was established ($V_{s,exp}^*$) and defined as V_{test} for a member with stirrups less the V_{test} magnitude for a comparable specimen without stirrups. The stirrup efficiency relative to Eq. (2) from the ACI 318 model was then evaluated with reference to a normalized efficiency ratio ($V_{s,exp}^*/V_{s,ACI}$). It is assumed in this study that changes

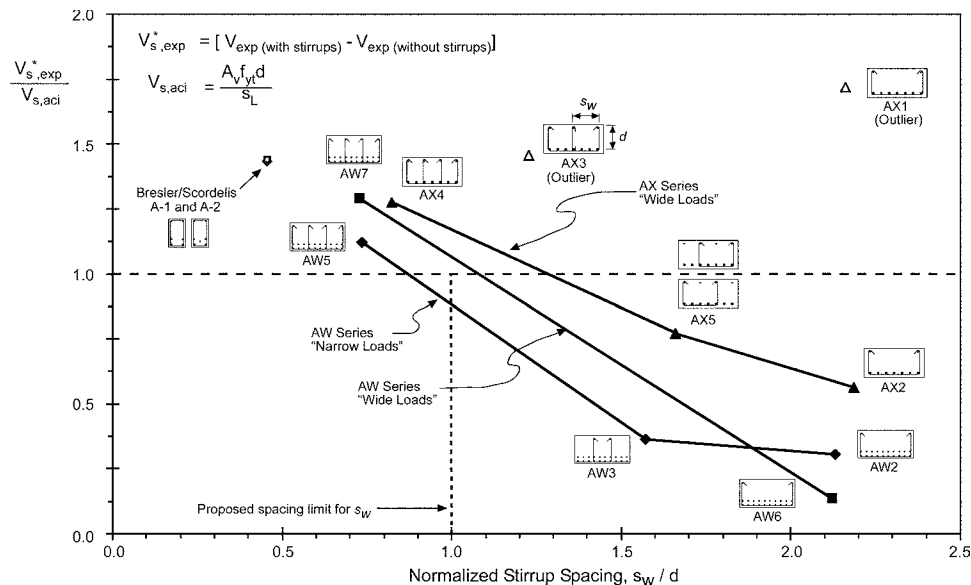


Fig. 10—Influence of stirrup leg spacing across width on effectiveness of shear reinforcement.

in the test-to-model ratio for geometrically identical members with identical reinforcement ratios result from changes in the shear reinforcement pattern.

Stirrup efficiency values for specimens reported in this paper are presented in Tables 1 and 2. All V_{test} results were established at a critical section d from the face of the support plate, including the effect of self-weight. The results reported do not make an adjustment for f'_c because similar values were established for companion specimens. Figure 10 illustrates the relationship between the stirrup efficiency factor and the normalized spacing of stirrup legs across the specimen width. A similar trend of decreasing stirrup efficiency with increased transverse spacing is observed for specimens with either full-width or narrow load and support conditions. When the transverse spacing exceeded approximately d for the AW series, the stirrup efficiency ratio was below 1.0. These are consistent with results reported by Serna-Ros et al.¹³ for much thinner members ($d = 206$ mm [8.1 in.]), and having shear reinforcement ratios approximately 50% higher than the AW and AX specimens.

Specimens in the AW and AX series represent wide members with large b_w/d and s_w/d ratios. For comparison with more traditional laboratory tests with smaller b_w/d and s_w/d ratios, often cited test data from Bresler and Scordelis²⁰ is also shown in Fig. 10. Specimens A-1 and A-2 had shear reinforcement ratios of $A_v f_y / b_w s \sim 0.33$ MPa (47 psi), s_w/d and s_L/d ratios of approximately 0.46, ρ_w of 1.80% and 2.27%, a/d of 3.97 and 4.90, and effective depths of 460 mm (18 in.). The stirrup efficiency of Specimens A-1 and A-2 relative to the companion members without stirrups (OA-1 and OA-2) were 1.43 and 1.44, respectively, falling on the trend lines established from the AW and AX specimens reported in this paper.

Predictions of the nominal one-way shear capacity for each specimen in the current test program using Eq. (3) were also completed and compared against the maximum shear force determined from the tests (Tables 1 and 2). The model provided as Eq. (3) resulted in V_{test}/V_n shear capacity prediction ratios greater than 1.0 for members with well-distributed web reinforcement (AW5, AW7, AX3, and AX4). Because there was little increase in shear capacity observed for members with wider stirrup leg spacing compared with

geometrically similar members without web reinforcement, the V_{test}/V_n ratio was below 1.0 for members AW2, AW3, and AW6. The ratio was only slightly above 1.0 for the thinner specimens with large s_w/d ratios (AX2 and AX5). In general, the test-to-model ratio for shear capacity decreased as the normalized stirrup spacing increased. From the V_{test}/V_n trend established by these results, a maximum stirrup spacing of d would ensure that V_{test}/V_n was above 1.0.

The use of narrow bearing plate sizes at the load and support locations reduced the comparable test-to-model predictions, as shown in Fig. 10. The influence of bearing plate size has been studied by several researchers^{3,7,13,21,22} and methods to account for its influence in capacity models have been provided elsewhere.^{3,13} The present study examines the full-width load and support case, which would represent the practical case, once corrections for load and support widths have been completed. The trends of decreased stirrup efficiency and decreased V_{test}/V_n for increased s_w/d in the current test program are similar, regardless of the load or support condition.

Recommended spacing limit for s_w

The influence of s_w on the shear capacity permits the establishment of design guidelines for maximum spacing of web reinforcement legs across the member width. Design limits must ensure that safe structures are always produced. From a design context, a quantity of web reinforcement would be selected assuming full efficiency. The current study considered the maximum leg spacing across the width at which the overall quality of the existing shear capacity model would not be unduly diminished. Spacing limits were assessed based on a fraction of the member depth, the applied shear stress, and an absolute value.

Maximum spacing of d across the width—For the specimens presented in Fig. 10, the trend observed for specimens with full width loads and supports will give stirrup efficiency ratios greater than 1.0, provided that s_w remains smaller than approximately d . Furthermore, this limit will result in V_{test}/V_n ratios greater than 1.0.

Absolute spacing of 600 mm (24 in.)—Maximum absolute dimensions should be specified for s_w to cater to very thick slabs or wide beams. The largest members available for

systematic validation are the 590 mm (23.2 in.) deep specimens in the current study. Moreover, very limited data are available for members with different geometrical ratios (b_w/d , a/d , b_w/a). In view of the limited data, an upper limit of 600 mm (24 in.) for spacing across the width is recommended, which is the same as the upper limit defined by ACI 318-08 for spacing in the longitudinal direction. A review of this limit should be completed as new tests data are developed for large, wide members with web reinforcement.

Spacing reduction in high shear stress regions—The tests described previously, from which these limits were developed, all contained relatively low web reinforcement ratios. In practice, most designs that might result in a low number of web reinforcement legs of small size are expected to fall in this range. At higher shear levels, the greater total quantity of web reinforcement required would permit a designer to use a larger number of small-diameter legs, thus giving a well-distributed condition. Because members subject to higher shear stresses have a greater proportion of their total shear strength from the stirrup contribution (V_s), it is essential that a high stirrup efficiency factor is achieved. Furthermore, members subject to high shear stresses are expected to be more heavily cracked at failure, emphasizing the importance of ensuring that crack widths and crack propagation are adequately controlled to maintain the shear transfer modes assumed by the V_c component of Eq. (3). Because of limited data in this area, it is recommended that each of the aforementioned spacing guidelines be reduced by 1/2 when the nominal shear stress on the section exceeds $0.42\sqrt{f'_c}$ MPa ($5\sqrt{f'_c}$ psi). This adjustment is consistent with the use of reduced longitudinal spacing limits in ACI 318-08 for members subject to high shear stresses. Furthermore, it is consistent with the recommendations of Anderson and Ramirez.⁸ Additional testing of large wide members subjected to high shear stresses may allow future review of this reduced spacing requirement.

CONCLUSIONS

The following conclusions can be drawn from this investigation of shear strength influences from web reinforcement configurations in wide reinforced concrete members:

1. The effectiveness of the shear reinforcement decreases as the spacing of web reinforcement legs across the width of a member increases;
2. The use of few web reinforcement legs, even when widely spaced up to a distance of approximately $2d$, has been shown to decrease the brittleness of the failure mode compared with a geometrically similar member without web reinforcement;
3. For a wide, simply-supported member with a central concentrated load, the distribution of strains in the longitudinal reinforcement varies across the member width. Furthermore, this distribution changes from that of typically higher strains in the outer bars at midspan to higher strains in the middle bars near the supports, but the pattern may be influenced by the support geometry; and
4. To ensure that the shear capacity of all members with web reinforcement are adequate when designed according to ACI 318-08, the transverse spacing of web reinforcement should be limited to the lesser of: a) the effective member depth d ; and b) 600 mm (24 in.). These limits should be

reduced by 1/2 when the nominal shear stress exceeds $0.42\sqrt{f'_c}$ MPa ($5\sqrt{f'_c}$ psi).

ACKNOWLEDGMENTS

The experimental research described in this paper was funded by the Natural Sciences and Engineering Research Council of Canada.

REFERENCES

1. Lubell, A.; Sherwood, T.; Bentz, E.; and Collins, M. P., "Safe Shear Design of Large, Wide Beams," *Concrete International*, V. 26, No. 1, Jan. 2004, pp. 66-78.
2. Sherwood, E. G.; Lubell, A. S.; Bentz, E. C.; and Collins, M. P., "One-Way Shear Strength of Thick Slabs and Wide Beams," *ACI Structural Journal*, V. 103, No. 6, Nov.-Dec. 2006, pp. 794-802.
3. Lubell, A. S., "Shear in Wide Reinforced Concrete Members," PhD dissertation, University of Toronto, Toronto, ON, Canada, May 2006, 455 pp.
4. Collins, M. P., and Kuchma, D., "How Safe Are Our Large, Lightly Reinforced, Concrete Beams, Slabs and Footings?" *ACI Structural Journal*, V. 96, No. 4, July-Aug. 1999, pp. 482-490.
5. ACI Committee 318, "Building Code Requirements for Structural Concrete (ACI 318-08) and Commentary," American Concrete Institute, Farmington Hills, MI, 2008, 465 pp.
6. Kani, G. N. J., "How Safe are Our Large Concrete Beams?" *ACI JOURNAL, Proceedings* V. 64, No. 3, Mar. 1967, pp. 128-142.
7. Leonhardt, F., and Walther, R., "The Stuttgart Shear Tests 1961," *Translation* No. 111, Cement and Concrete Association, London, UK, 1964, 134 pp.
8. Anderson, N. S., and Ramirez, J. A., "Detailing of Stirrup Reinforcement," *ACI Structural Journal*, V. 86, No. 5, Sept.-Oct. 1989, pp. 507-515.
9. AASHTO, "AASHTO LRFD Bridge Design Specifications and Commentary," third edition, American Association of State Highway Transportation Officials, Washington, DC, 2004, 1264 pp.
10. Eurocode 2, "Design of Concrete Structures—Part 1-1: General Rules and Rules for Buildings (EN1992-1-1)," European Committee for Standardization, Brussels, Belgium, Dec. 2004, 225 pp.
11. CSA, "Design of Concrete Structures (CAN/CSA A23.3-04)," Canadian Standards Association, Mississauga, ON, Canada, 2004.
12. Hsiung, W., and Frantz, G. C., "Transverse Stirrup Spacing in R/C Beams," *Journal of Structural Engineering*, ASCE, V. 111, No. 2, Feb. 1985, pp. 353-362.
13. Serna-Ros, P.; Fernandez-Prada, M. A.; Miguel-Sosa, P.; and Debb, O. A. R., "Influence of Stirrup Distribution and Support Width on the Shear Strength of Reinforced Concrete Wide Beams," *Magazine of Concrete Research*, V. 54, No. 3, June 2002, pp. 181-191.
14. Zheng, L., "Shear Tests to Investigate Stirrup Spacing Limits," MASC thesis, Department of Civil Engineering, University of Toronto, Toronto, ON, Canada, 1989, 161 pp.
15. Monteleone, V., "Headed Shear Reinforcement in Shell Elements Under Reversed Cyclic Loading," MASC thesis, Department of Civil Engineering, University of Toronto, Toronto, ON, Canada, 1993, 245 pp.
16. Joint ACI-ASCE Committee 426, "The Shear Strength of Reinforced Concrete Members," *Journal of the Structural Division*, ASCE, V. ST6, June 1973, pp. 1091-1187.
17. Joint ACI-ASCE Committee 326, "Shear and Diagonal Tension," *ACI JOURNAL*, V. 59, No. 1, 2, and 3, Jan., Feb., and Mar. 1962, pp. 1-30, 277-344, and 352-396.
18. Ritter, W., "Die Bauweise Hennebique (Construction Techniques of Hennebique)," *Schweizerische Bauzeitung*, Zurich, V. 33, No. 7, Feb. 1899, pp. 59-61.
19. Mörsch, E., "Concrete-Steel Construction (Der Eisenbetonbau)," Translation of the Third German Edition by E.P. Goodrich, McGraw Hill, New York, 1909, 368 pp.
20. Bresler, B., and Scordelis, A. C., "Shear Strength of Reinforced Concrete Beams," *ACI JOURNAL, Proceedings* V. 60, No. 1, 1963, pp. 51-72.
21. Regan, P. E., and Rezai-Jorabi, H., "Shear Resistance of One-Way Slabs Under Concentrated Loads," *ACI Structural Journal*, V. 85, No. 2, Mar.-Apr. 1988, pp. 150-157.
22. Diaz de Cossio, R., discussion on "Shear and Diagonal Tension," *ACI JOURNAL, Proceedings* V. 59, No. 9, Sept. 1962, pp. 1323-1332.